Sudden spontaneous acceleration and deceleration of gap-acoustic solitons

Richard S. Tasgal,* R. Shnaiderman, and Y. B. Band

Department of Chemistry and Department of Electro-Optics, and the Ilse Katz Center for Nano-Science, Ben-Gurion University of the Negev, Beer-Sheva 84105, Israel
**Corresponding author: tasgal@bgu.ac.il*

Received November 5, 2009; revised February 9, 2010; accepted February 21, 2010; posted March 23, 2010 (Doc. ID 119568); published April 28, 2010

Gap-acoustic solitons (GASs) are stable pulses that exist in nonlinear Bragg waveguides. They are a mathematical generalization of gap solitons, in which the model includes the dependence of the refractive index on the material density. We derive unified dynamical equations for gap solitons along with Brillouin scattering, which also results from the dependence of the refractive index on the material density. We find accurate values of the coefficients for fused silica. The analysis of the GAS conserved quantities—Hamiltonian, momentum, photon energy (or number of photons), and material mass—shows dramatic differences compared to the model neglecting the dependence of the refractive index on the material density. In particular, subsonic GASs in fused silica have far more momentum at low velocities than at high velocities. The dependence of the GAS momentum on velocity due to acoustic effects is dramatic up to approximately 1% of the speed of light. These momentum-connected effects mean that instability of a slow GAS may make it suddenly accelerate to high speeds, and also that an unstable high-speed GAS can abruptly decelerate to close to zero velocity. The predictions are confirmed by a direct numerical simulation.

OCIS codes: 060.4370, 060.3735, 230.1040, 190.5530, 290.5830, 190.3100.

1. INTRODUCTION

A gap-acoustic soliton (GAS) is an optical and acoustic structure that can exist in an optical waveguide with a Bragg grating. The GAS is a generalization of the gap soliton [1–4], but includes the dependence of the refractive index on the density of the material. Physically, this dependence is always present, but is not always included in the mathematical description. The correct interaction between sound and light not only provides generalized soliton solutions, but also allows an accurate description of other interactions between light and sound.

The first gap soliton paper did not use the phrase "gap soliton," but rather referred to the equations as the massive Thirring model (MTM) [1]. The solutions were solitons in the strictest sense—the system was shown to be integrable by the inverse scattering method [2,3]. The soliton frequencies are in the gap between the frequencies of the two continuous wave (cw) solutions. However, the soliton frequencies *are not all* between the *maximum* of the lower cw band and the *minimum* of the upper cw band. For this reason, some authors prefer the term "Bragg soliton" (see, e.g., [4]).

Independently of the mathematical discovery of gap solitons, a qualitative description and prediction of the still theoretical optical gap solitons was made in [5]. Exact analytical forms for optical gap solitons were found for a nonlinearity with self-phase modulation in addition to cross-phase modulation. Reference [6] found the solutions in the exact middle of the bandgap, and [7] found the full family of gap soliton solutions. This is not a completely integrable system, and the pulses are solitons in the broader sense but not in the narrower sense; so they are not guaranteed to have the stability MTM solitons.

All GASs (as well as all optical gap solitons) are a form of slow (or stopped) light, in the sense that the soliton velocity is slower than the group velocity of light in the medium. Optical gap solitons have been realized experimentally with velocities as low as 23% of the group velocity (or 16% of the speed of light in vacuum) [8]. This may be compared and contrasted with light that is slow in the sense that the group velocity is significantly less than the phase velocity in the medium, generally due to a steep slope of the index of refraction with respect to the frequency in the vicinity or a resonance [9–15].

The stability of gap solitons beyond the completely integrable MTM limit (optical gap solitons have nonzero self-phase modulation, and so are not MTM) was not immediately clear. Reference [6] showed one direct numerical simulation of a gap soliton collision in which the individual gap solitons were stable, and the solitons emerged from a collision intact but perturbed. Reference [16] performed variational model calculations of optical gap solitons, which showed some regions where excited modes exist and other regions with instabilities. References [17–19] rigorously showed that optical gap solitons are stable in the top half of the bandgap and unstable in most of the bottom half of the bandgap. Reference [20] generalized the optical gap soliton equations to a model that includes the dependence of the index of refraction on the density of the material and the phonon-photon interactions that result from it; that is, the effect of light on low wave number acoustic waves [21], and vice versa, was included in the model, and generalized "gap-acoustic soliton" solutions were found [20]. The GASs are similar to optical gap solitons, but they exhibit many intriguing novel dynamical properties, especially when the soliton

velocities are small. A subset of the GAS model, without self-phase modulation, was studied in [22]. Reference [23] found solitons in a system with two short-wavelength light fields interacting with a long-wavelength electromagnetic field; the interaction there is different from that in [20] or in this work, but there are family resemblances. Reference [24] looked at the interaction of light beams, i.e., propagation in space rather than in time, with sound waves via electrostriction.

The dependence of the index of refraction on the density of the material is physically universal. Light interacts with sound waves because the energy density of light is proportional to the refractive index [25] which, in turn, depends on the density. The interaction between light and high wave number acoustic waves—approximately twice the wave numbers of light—is called Brillouin scattering [26], and the interaction between light and low wave number acoustic waves is generally referred to as electrostriction [27]. Notwithstanding different nomenclatures, the two effects have the same physical source. Brillouin scattering can cause light in a medium to create its own Bragg reflector, and if the input light is a pulse then the outgoing reflected pulse can be shortened by this effect [27–31].

Phonon viscosity can be caused by elastic anharmonicity, Rayleigh scattering, vibrational relaxation, and impurities in the medium [32]; it scales approximately as the square of the wave number. It gives rise to damping of acoustic waves and results in a finite frequency spread for Brillouin scattering. Phonon viscosity has been considered in some detail for propagation of trains of optical solitons and non-solitonic pulses in media without a Bragg lattice [33,34].

This work builds on top of [20], expanding on the physically most important realization the fused silica. We also generalize the model [20] to cover high wave number (Brillouin) acoustic wave interactions as well as low wave number (electrostrictive) acoustic waves, including the derivation of the governing equations for both acoustic waves in a unified manner.

The outline of this paper is as follows. Section 2 gives the governing equations for the relevant electromagnetic and acoustic fields, along with the values of the coefficients for the case of fused silica. The derivation of the governing equations is given in the Appendix A. Section 3 details the general properties of this system. Section 4 gives the soliton solutions and outlines the stability properties. Section 5 takes a closer look at the conserved and quasi-conserved quantities of the system. Section 6 predicts abrupt acceleration and sudden deceleration to zero velocity, based on the conserved quantities, and confirms the predictions with direct numerical simulations. Section 7 contains summary and conclusion.

2. GOVERNING EQUATIONS AND PHYSICAL PARAMETERS

GASs exist in a nonlinear optical waveguide with a Bragg grating along the axis of the fiber or in a bulk medium if the propagating beams are wide enough so that there are no complex transverse dynamics. Let us take the Bragg grating as uniform, with period λ_{Bragg} and amplitude of the variation in the index of refraction Δn,

$$n(z) = n(\omega, W) + \Delta n \cos(2\pi z/\lambda_{\mathrm{Bragg}}), \tag{1}$$

where the baseline refractive index implicitly allows the dependence on the frequency of light (ω) and on the density of the material [$W(z,t)$]. Light will be in resonance with the grating if it has a wavelength in the medium twice as long as the Bragg wavelength. At light frequencies in resonance with the Bragg grating, forward-moving light will be reflected backward, and backward-moving light will be reflected forward. The result will be a bandgap in the frequency at plus and minus the resonant wave number. The electric field can then be described by two slowly varying envelopes (SVEs) about carrier waves at the same frequency and plus or minus the corresponding resonant wave number. Light interacts with phonons due to the dependence of the refractive index on the density of the medium, which is universal, even though the interaction may sometimes be omitted from models of the system. Phonons can interact with the two SVEs if their wave numbers are twice the wave number of light (or, equivalently, the phonon wavelengths are half the wavelength of the light's carrier wave). Additionally, phonons can interact with light if their wave numbers are close to zero, with a distance scale similar to the distance scales of the envelopes of the light intensity. We consider only low- and high-frequency longitudinal acoustic modes, even though, in general, additional modes are supported. A waveguide has at least three acoustic modes: one longitudinal (also called compression or dilation) mode and two transverse (shear) modes. If the fiber is thick, there may be additional transverse acoustic modes, and thus be an acoustically multi-mode fiber [35,36]. We assume that one of the acoustic modes is the most important and neglect the others, because the analysis should begin with the most basic acoustic effects and defer to study of multi-mode and other higher-order effects. For *trains* of pulses, acoustic waves traveling in a direction normal to the fiber axis, and reflecting off the fiber circumference, have been invoked to account for inter-pulse interactions in communication fibers [21,34]. This multi-mode effect may be neglected here because it is a higher-order perturbation, and it may not be relevant at all for the individual pulses that we deal with. Figure 1 is a schematic illustration of a fiber waveguide with a periodically varying refractive index with light and sound waves propagating within it. A Bragg grating can be produced by doping the waveguide with ions and imprinting a periodic variation in the index of refraction with ultraviolet light [28].

The derivation of the equations for this system is given in the Appendix A. The electric field and the material density (phonon field) in terms of nontrivial SVEs,

$$\begin{aligned} E(z,t) = {} & u(z,t)\exp[i(k_0 z - \omega_0 t)] + v(z,t)\exp[-i(k_0 z + \omega_0 t)] \\ & + u(z,t)^*\exp[-i(k_0 z - \omega_0 t)] + v(z,t)^*\exp[i(k_0 z \\ & + \omega_0 t)], \end{aligned} \tag{2a}$$

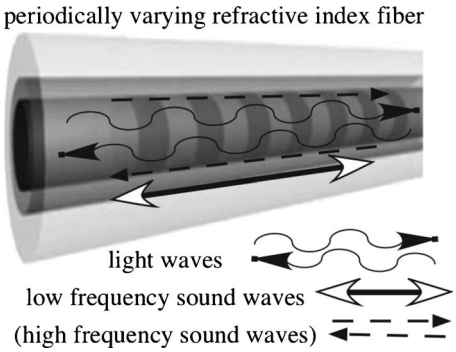

Fig. 1. Schematic illustration of a fiber with a periodically varying refractive index. Light and sound waves propagate in the fiber. Photons are shown as wavy lines with arrows indicating the direction of motion; the low-frequency phonons are shown as a solid line with double-sided arrows, and high-frequency phonons are shown as dashed lines with arrows.

$$W(z,t) = w_0(z,t) + w_u(z,t)\exp[2ik_0(z-\beta_s t)] + w_v(z,t)\exp[-2ik_0(z+\beta_s t)] + w_u(z,t)^*\exp[-2ik_0(z-\beta_s t)] + w_v(z,t)^*\exp[2ik_0(z+\beta_s t)], \tag{2b}$$

obey the dynamical equations,

$$0 = ik_0' u_t + iu_z + \kappa v + \frac{2\pi(\omega_0/c)^2}{k_0}3\chi^{(3)}(|u|^2+2|v|^2)u + \chi_{es}[w_0 u + \exp(-2ik_0\beta_s t)w_u v + \exp(2ik_0\beta_s t)w_v^* v], \tag{3a}$$

$$0 = ik_0' v_t - iv_z + \kappa u + \frac{2\pi(\omega_0/c)^2}{k_0}3\chi^{(3)}(2|u|^2+|v|^2)v + \chi_{es}[w_0 v + \exp(2ik_0\beta_s t)w_u^* u + \exp(-2ik_0\beta_s t)w_v u], \tag{3b}$$

$$0 = w_{0,tt} - \beta_s^2 w_{0,zz} - \Gamma w_{0,tzz} + \lambda_{es}(|u|^2+|v|^2)_{zz}, \tag{3c}$$

$$0 = iw_{u,t} + i\beta_s w_{u,z} + i(2k_0^2\Gamma)w_u + \frac{k_0\lambda_{es}}{\beta_s}\exp(2ik_0\beta_s t)uv^*, \tag{3d}$$

$$0 = iw_{v,t} - i\beta_s w_{v,z} + i(2k_0^2\Gamma)w_v + \frac{k_0\lambda_{es}}{\beta_s}\exp(2ik_0\beta_s t)u^*v, \tag{3e}$$

where the values of the coefficients in terms of basic physical quantities are

$$n = n(\omega,W) + \Delta n\,\cos(2k_0 z), \tag{4a}$$

$$k(\omega,W) = n(\omega,W)\omega/c, \tag{4b}$$

$$k_0 = k(\omega_0,W_0), \tag{4c}$$

$$k_0' = v_g^{-1} = \frac{\partial}{\partial\omega}k(\omega,W)|_{\omega=\omega_0,W=W_0}, \tag{4d}$$

$$\chi_s = 3\chi^{(3)}(\omega_0;\omega_0,-\omega_0,\omega_0), \tag{4e}$$

$$\chi_x = 6\chi^{(3)}(\omega_0;\omega_0,-\omega_0,\omega_0), \tag{4f}$$

$$\kappa = \frac{\omega_0}{c}\frac{\Delta n}{2}, \tag{4g}$$

$$\chi_{es} = \frac{\omega_0}{c}\frac{\partial n}{\partial W}, \tag{4h}$$

$$\lambda_{es} = \frac{n(\omega_0)}{2\pi}W\frac{\partial n}{\partial W}. \tag{4i}$$

The more basic underlying physical properties—the refractive index $n(\omega)$, the magnitude of the periodic variation of the refractive index Δn (for the Bragg grating), the Kerr nonlinearity $\chi^{(3)}(\omega;\omega,-\omega,\omega)$, the material density W, the slope of the refractive index with density $\partial n/\partial W$, the speed of sound in the waveguide β_s, and the phonon viscosity in the waveguide Γ—must in the end be found experimentally.

Some of the physics can be more clearly illustrated by defining two new variables that are combinations of forward- and backward-moving waves,

$$\kappa_{\mathrm{Brill}} \equiv \chi_{es}[\exp(-2ik_0\beta_s t)w_u + \exp(2ik_0\beta_s t)w_v^*], \tag{5a}$$

$$\mathcal{L}_{\mathrm{Brill}} \equiv \chi_{es}[\exp(-2ik_0\beta_s t)w_u - \exp(2ik_0\beta_s t)w_v^*]. \tag{5b}$$

Using the variables (5), the dynamical equations (3) are

$$0 = ik_0' u_t + iu_z + (\kappa+\kappa_{\mathrm{Brill}})v + \frac{2\pi(\omega_0/c)^2}{k_0}3\chi^{(3)}(|u|^2+2|v|^2)u + \chi_{es}w_0 u, \tag{6a}$$

$$0 = ik_0' v_t - iv_z + (\kappa+\kappa_{\mathrm{Brill}})^* u + \frac{2\pi(\omega_0/c)^2}{k_0}3\chi^{(3)}(2|u|^2+|v|^2)v + \chi_{es}w_0 v, \tag{6b}$$

$$0 = w_{0,tt} - \beta_s^2 w_{0,zz} - \Gamma w_{0,tzz} + \lambda_{es}(|u|^2+|v|^2)_{zz}, \tag{6c}$$

$$0 = -\left(\frac{\partial}{\partial t} + 2k_0^2\Gamma\right)\kappa_{\mathrm{Brill}} + \beta_s\left(-2ik_0 + \frac{\partial}{\partial z}\right)\mathcal{L}_{\mathrm{Brill}}, \tag{6d}$$

$$0 = -\left(\frac{\partial}{\partial t} + 2k_0^2\Gamma\right)\mathcal{L}_{\mathrm{Brill}} + \beta_s\left(-2ik_0 - \frac{\partial}{\partial z}\right)\kappa_{\mathrm{Brill}} + 2ik_0\beta_s\left(\frac{\chi_{es}\lambda_{es}}{\beta_s^2}\right)u^* v. \tag{6e}$$

This form eliminates explicit time-dependencies and is more suitable for a direct numerical simulation of the partial differential equations. Moreover, it shows more directly how the Brillouin phonons can act as Bragg scatterers.

Let us examine some typical physical coefficients. The most common waveguide material is fused silica. For simplicity, we take the values of the medium in bulk since waveguiding effects are non-universal and the bulk values are suitable as a baseline. Consider light at a wave-

length of $\lambda_0=0.8$ or 1.55 μm. The refractive index in the region between those wavelengths is close to $n=1.45$. The nonlinear coefficients can be found in Fig. 2 of [37], which plots the Kerr nonlinear coefficient of the intensity n_2^I, defined by $n(I)=n(I=0)+n_2^I I$, where $I=(2\pi)^{-1}n(\omega)c|E(\omega)|^2$ is the intensity, $n_2^I(0.8\ \mu\text{m})=2.8\times10^{-16}$ cm^2/W, and $n_2^I(1.55\ \mu\text{m})=2.65\times10^{-16}$ cm^2/W. To obtain the self- and cross-phase modulation coefficients, we first want to express this in terms of the third-order susceptibility. Using Gaussian units, the nonlinear polarization is

$$P_{\text{NL}}(x,t)=\int\int\int \chi^{(3)} \times(t;t_1,t_2,t_3)E(x,t_1)E(x,t_2)E(x,t_3)dt_1dt_2dt_3.$$

For an electric field at a frequency of approximately ω_0, $E(x,t)=u(x,t)\exp(ik_0z-i\omega_0t)+\text{c.c.}$, where $u(x,t)$ is a SVE, the nonlinear polarization is $P_{\text{NL}}(x,t)\approx 3\chi^{(3)}(\omega_0;\omega_0,-\omega_0,\omega_0)|u(x,t)|^2u(x,t)$, or in the frequency space, $P_{\text{Kerr}}(\omega)=3\chi^{(3)}(\omega_0;\omega_0,-\omega_0,\omega_0)|E(\omega_0)|^2E(\omega_0)$. The self- and cross-phase modulation coefficients come from the third-order susceptibility [Eqs. (4e) and (4f)], which, for the values above, is $\chi^{(3)}(\omega_0;\omega_0,-\omega_0,\omega_0)=(12\pi^2)^{-1}n(\omega_0)^2cn_2^I$; at 0.8 μm, $\chi^{(3)}=1.5\times10^{-14}$ cm s^2/g, and at 1.55 μm, $\chi^{(3)}=1.4\times10^{-14}$ cm s^2. The self- and cross-phase modulation coefficients are then $\chi_s(0.8\ \mu\text{m})=4.5\times10^{-14}$ cm s^2/g and $\chi_x(0.8\ \mu\text{m})=9.0\times10^{-14}$ cm s^2/g, or $\chi_s(1.55\ \mu\text{m})=4.2\times10^{-14}$ cm s^2/g and $\chi_x(1.55\ \mu\text{m})=8.4\times10^{-14}$ cm s^2/g. Alternatively, the units may be expressed as cm s^2/g $=(\text{cm/statvolt})^2=[(10^4\ \text{m/s})/c]^2(\text{m/V})^2$. It may also be helpful to express the self-phase modulation coefficient directly in terms of the measured nonlinear coefficient in [37]: $[2\pi(\omega_0/c)^2/k_0]\chi_s=n_2^In(\omega_0)\omega_0/(2\pi)$. Reference [32] measures the optical and mechanical properties of bulk fused silica. Values which we can use as a typical baseline are the material density $W=2.2$ g/cm^3, the refractive index versus density $\partial n/\partial W=0.2$ cm^3/g, and the speed of sound $\beta_s=5.9$ km/s. The phonon viscosity Γ is a function of the Brillouin linewidth ($\Delta\nu_B$) and the wavelength (λ_B) at which it is measured. Equating the decay time of the Brillouin phonons $\tau_B=(\pi\Delta\nu_B)^{-1}$ [28] with the decay distance from Eqs. (3), $\tau_B=(2k_B^2\Gamma)^{-1}$, gives $\Gamma=(8\pi)^{-1}\lambda_B^2\nu_B$. For $\nu_B\approx50$ MHz measured at $\lambda_B=0.5893$ μm [32], the phonon viscosity is $\Gamma=6.9\times10^{-7}$ m^2/s. Lastly, the strength of the Bragg grating imprinted onto the waveguide, Δn, cannot be said to have any typical value, but can take vastly different values in different waveguides.

Waveguides can have significantly different optical and acoustic properties than the bulk [35,36,38–45]. This is partly due to variations in the transverse cross-section of the light intensity and partly due to the composite nature of fibers—interfaces between the core and cladding are especially sensitive to opto-mechanical affects and can also absorb acoustic energy. For example, [39,40] measured the contribution of electrostriction to the Kerr effect for linear light in an optical fiber at low frequencies ($\chi_{es}\lambda_{es}/\beta_s^2$). This factor is obtained by eliminating the time derivatives in Eq. (3c) and substituting the acoustic deformation $w_0(z)=(\lambda_{es}/\beta_s^2)(|u|^2+|v|^2)$ back into the light propagation [Eqs. (3a) and (3b)]. Reference [39] found electrostriction to be equal to 19% of the fast (mainly electronic) contribution to the Kerr effect $[2\pi(\omega_0/c)^2/k_0]\chi_s$ [39], or 16% of the total Kerr effect, and [40] found different values for different fibers, using unpolarized light, including electrostrictive Kerr contributions a few times larger. By comparison, for bulk fused silica and linear polarized light at the wavelength of $\lambda_0=0.8$ μm, using the (typical) material coefficients above, the electrostrictive contribution to the Kerr coefficient is $\chi_{es}\lambda_{es}/\beta_s^2\approx0.46\times10^{-8}$ s^2/g, and the fast contribution to the Kerr coefficient is $[2\pi(\omega_0/c)^2/k_0]\chi_s=1.53\times10^{-8}$ s^2/g, giving an electrostrictive contribution of 30% of the fast nonlinearity or 23% of the total Kerr effect. At the wavelength of $\lambda_0=1.55$ μm, $\chi_{es}\lambda_{es}/\beta_s^2\approx0.24\times10^{-8}$ s^2/g, and the fast contribution to the Kerr coefficient is $[2\pi(\omega_0/c)^2/k_0]\chi_s=0.75\times10^{-8}$ s^2/g, giving an electrostrictive contribution of 32% of the fast nonlinearity or 24% of the total Kerr effect. In this instance, the expected contribution of electrostriction toward the Kerr effect at low frequencies in bulk fused silica is not so far from—in fact, surprisingly close to—the values measured in fibers. This is a confirmation of the qualitative and quantitative accuracies of the model herein.

3. LAGRANGIAN, HAMILTONIAN, AND CONSERVED QUANTITIES

The Bragg–Brillouin–Kerr system (3) can be written in terms of a Lagrangian density in the limit in which phonon viscosity vanishes, $\Gamma=0$,

$$\begin{aligned}\mathcal{L}=&\frac{i}{2}k_0'(u^*u_t-uu_t^*)+\frac{i}{2}k_0'(v^*v_t-vv_t^*)+\frac{i}{2}(u^*u_z-uu_z^*)\\&-\frac{i}{2}(v^*v_z-vv_z^*)+\kappa u^*v+\kappa^*uv^*+\frac{2\pi(\omega_0/c)^2}{k_0}\left[\frac{\chi_s}{2}(|u|^4\right.\\&\left.+|v|^4)+\chi_x|u|^2|v|^2\right]+\frac{\chi_{es}}{2\lambda_{es}}(r_t^2-\beta_s^2r_z^2)+\chi_{es}(|u|^2+|v|^2)r_z\\&+\frac{\chi_{es}\beta_s}{k_0\lambda_{es}}\frac{i}{2}[(w_u^*w_{u,t}-w_uw_{u,t}^*)+(w_v^*w_{v,t}-w_vw_{v,t}^*)]\\&+\frac{\chi_{es}\beta_s^2}{k_0\lambda_{es}}\frac{i}{2}[(w_u^*w_{u,z}-w_uw_{u,z}^*)-(w_v^*w_{v,z}-w_vw_{v,z}^*)]\\&+\chi_{es}\exp(-2ik_0\beta_st)(u^*vw_u+uv^*w_v)+\chi_{es}\exp(2ik_0\beta_st)\\&\times(u^*vw_v^*+uv^*w_u^*).\end{aligned}\tag{7a}$$

Here we have introduced a potential for the slowly varying phonon field,

$$r(z,t)\equiv\int_{z_0}^{z}w_0(z',t)dz',\tag{7b}$$

where z_0 is an arbitrary constant. A Hamiltonian H can be derived from this Lagrangian. It is a conserved quantity, and three additional conserved quantities exist; the conserved quantities are the Hamiltonian H, momentum P, photon energy N (also called the number of photons), and material mass M,

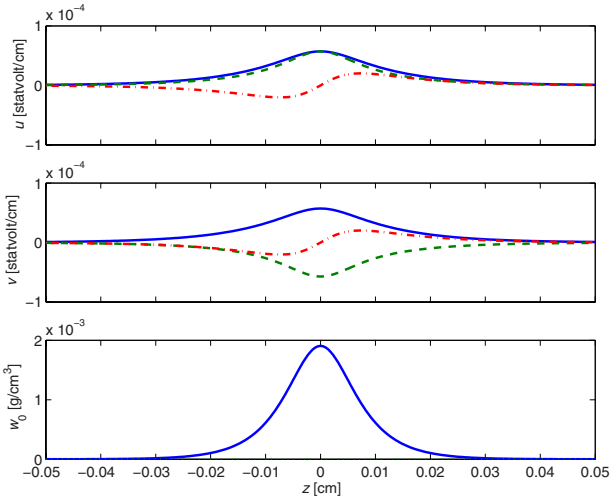

Fig. 2. (Color online) Quiescent (zero velocity, $\beta=0$) GAS, with frequency in the middle of the bandgap, $Q=\pi/2$. The physical parameters are typical of bulk fused silica, and the Bragg coefficient is $\kappa=90\ \mathrm{cm}^{-1}$. The top part of the figure shows the amplitude of the envelope u of the forward-moving electromagnetic wave, the middle part shows the envelope v of the backward-moving wave, and the bottom part shows the acoustic field (material density). Solid lines are for the magnitudes of the amplitudes, dashed lines for the real parts, and dotted lines are for the imaginary parts.

$$M = A\int_{-\infty}^{\infty} w_0 dz, \tag{8a}$$

$$N = \frac{n(\omega_0)^2}{4\pi}A\int_{-\infty}^{\infty}(|u|^2+|v|^2)dz, \tag{8b}$$

$$P = -\frac{n(\omega_0)^2}{4\pi\omega_0}A\int_{-\infty}^{\infty}\left\{\frac{i}{2}(u^*u_z - uu_z^* + v^*v_z - vv_z^*) + \frac{\chi_{es}}{\lambda_{es}k_0'}r_z r + \frac{\beta_s/k_0'}{2k_0\chi_{es}\lambda_{es}}\frac{i}{2}(\kappa_{\mathrm{Brill},z}\kappa_{\mathrm{Brill}}^* - \kappa_{\mathrm{Brill},z}^*\kappa_{\mathrm{Brill}} + \mathcal{L}_{\mathrm{Brill},z}\mathcal{L}_{\mathrm{Brill}}^* - \mathcal{L}_{\mathrm{Brill},z}^*\mathcal{L}_{\mathrm{Brill}})\right\}dz, \tag{8c}$$

$$H = \frac{n(\omega_0)^2}{4\pi\omega_0 k_0'}A\int_{-\infty}^{\infty}\left\{-\frac{i}{2}(u^*u_z - uu_z^* - v^*v_z + vv_z^*) - (\kappa + \kappa_{\mathrm{Brill}})u^*v - (\kappa+\kappa_{\mathrm{Brill}})^*uv^* - \frac{2\pi(\omega_0/c)^2}{k_0}\left[\frac{\chi_s}{2}(|u|^4+|v|^4) + \chi_x|u|^2|v|^2\right] + \frac{\chi_{es}}{2\lambda_{es}}(r_t^2+\beta_s^2 r_z^2) - \chi_{es}(|u|^2+|v|^2)r_z - \frac{\beta_s^2}{2k_0\chi_{es}\lambda_{es}}\frac{i}{2}(\kappa_{\mathrm{Brill},z}\mathcal{L}_{\mathrm{Brill}}^* - \kappa_{\mathrm{Brill},z}^*\mathcal{L}_{\mathrm{Brill}} - \kappa_{\mathrm{Brill}}\mathcal{L}_{\mathrm{Brill},z}^* + \kappa_{\mathrm{Brill}}^*\mathcal{L}_{\mathrm{Brill},z})\right\}dz. \tag{8d}$$

Here A is the area of the transverse cross-section of the guided mode. Actually, the most general conserved quantity corresponding to the invariance of the system with respect to an additive constant in $r(z,t)$ is not as in Eq. (8a), but $\int_{-\infty}^{\infty} r_t dz$ (with a multiplicative and an additive constant). Because the reference density w_0 in our model goes to zero at plus and minus infinities, we can define M as in Eq. (8a) without fear of divergence on an infinite domain. Note that H in Eq. (8d) is not all the physical energy in the system, but excludes a constant (N, the energy in the electromagnetic field) that does not affect the dynamics. If phonon viscosity is nonzero, the acoustic fields decay. The photon energy (or number of photons) N and the mass M remain constants of motion in the presence of phonon viscosity, but the momentum P and Hamiltonian H decay.

4. GAP-ACOUSTIC SOLITONS

If the Brillouin fields (w_u, w_v) and phonon viscosity (Γ) in Eqs. (3) are neglected, there is a family of GAS solutions [20],

$$u(z,t) = \sqrt{\kappa\gamma(1+\beta k_0')}\alpha\ \mathrm{sn}\,Q\ \mathrm{sech}\left(\zeta\ \mathrm{sn}\,Q - \frac{i}{2}Q\right)\exp[i\theta(\zeta) - i\tau\ \mathrm{cn}\,Q], \tag{9a}$$

$$v(z,t) = -\sqrt{\kappa^*\gamma(1-\beta k_0')}\alpha\ \mathrm{sn}\,Q\ \mathrm{sech}\left(\zeta\ \mathrm{sn}\,Q + \frac{i}{2}Q\right)\exp[i\theta(\zeta) - i\tau\ \mathrm{cn}\,Q], \tag{9b}$$

$$w(z,t) = \frac{\lambda_{es}}{\beta_s^2-\beta^2}\frac{\gamma|\kappa|(4|\alpha|^2)\mathrm{sn}^2\,Q}{\cosh(2\zeta\ \mathrm{sn}\,Q) + \mathrm{cn}\,Q}, \tag{9c}$$

where

$$\theta(\zeta) = \beta k_0'\gamma^2(4|\alpha|^2)\left[\frac{2\pi(\omega_0/c)^2}{k_0}\chi_s + \frac{\chi_{es}\lambda_{es}}{\beta_s^2-\beta^2}\right]\tan^{-1}[\tanh(\zeta\ \mathrm{sn}\,Q)\tan(Q/2)], \tag{10a}$$

$$\alpha = \left(\frac{2\pi(\omega_0/c)^2}{k_0}\{\chi_x + \chi_s\gamma^2[1+(\beta k_0')^2]\} + 2\gamma^2\frac{\chi_{es}\lambda_{es}}{\beta_s^2-\beta^2}\right)^{-1/2}, \tag{10b}$$

$$\tau \equiv \gamma|\kappa|(t/k_0' - \beta k_0' z), \tag{10c}$$

$$\zeta \equiv \gamma|\kappa|(z-\beta t), \tag{10d}$$

$$\gamma \equiv [1-(\beta k_0')^2]^{-1/2}, \tag{10e}$$

and α must be real-valued. In the quiescent limit ($\beta=0$), these are also solutions for nonzero phonon viscosity ($\Gamma>0$). The solitons (9) and (10) have two essential intrinsic parameters: Q and β. The soliton parameter Q resembles a similar parameter in the family of the ordinary gap soli-

tons; it takes values $0<Q<\pi$ and determines the soliton width [full width at half-maximum equals $\cosh^{-1}(2+\cos Q)/(\gamma|\kappa|\sin Q)$], the peak intensity, and the frequency [in the rest frame, $(\gamma|\kappa|/k_0')\cos Q$]. The frequency in the frame moving with the soliton *is not* generally equal to $(|\kappa|/k_0')\cos Q$ because the group velocity in a medium is not equal to the speed of light in vacuum ($k_0'c \neq 1$). The soliton velocity β may take any value up to the group velocity of light in the medium ($|\beta|<1/k_0'$), except for a range of slightly supersonic gap solitons ($|\beta| \notin [\beta_s,\beta_{\rm cr}]$), where

$$\beta_{\rm cr}^2=\frac{1}{2(k_0')^2}\frac{\chi_x+\chi_s}{\chi_x-\chi_s}+\frac{\beta_s^2}{2} - \sqrt{\left(\frac{\chi_x+\chi_s}{(\chi_x-\chi_s)2(k_0')^2}-\frac{\beta_s^2}{2}\right)^2-\frac{k_0}{2\pi(\omega_0/c)^2}\frac{2\chi_{es}\lambda_{es}/(k_0')^2}{\chi_x-\chi_s}}. \tag{11}$$

At the typical coefficients given above for bulk fused silica, the critical velocities at the two frequencies are $\beta_{\rm cr}(0.8\ \mu{\rm m})=6.46\ {\rm km/s}=1.10\beta_s$ and $\beta_{\rm cr}(1.55\ \mu{\rm m})=6.50\ {\rm km/s}$. Bright supersonic as well as subsonic solitons exist if the critical velocity $\beta_{\rm cr}$ is less than the speed of light in the medium, which will hold in all but very exotic circumstances. (The equations suggest the existence of a dark soliton [46] in the supersonic region $\beta_s<\beta<\beta_{\rm cr}$, but we choose to limit this paper to bright solitons.)

The GASs (9) and (10) reduce to standard gap solitons [7] in the limit of zero electrostriction ($\chi_{es}=\lambda_{es}=0$). There are resemblances to solitons in the Zakharov system [47–52], in that both contain dispersive equations coupled to a non-dispersive equation, interaction with the non-dispersive field changes the amplitude of the soliton, and the non-dispersive field takes a profile the same shape as the soliton intensity; furthermore, like GASs, Zakharov solitons have different dynamics above and below the velocity of the non-dispersive field, with instabilities for the faster solitons. Below the speed of sound, the accompanying phonon pulse is a compression, and above the speed of sound the phonon pulse is a rarefaction. The amplitude of the acoustic pulse goes to zero when the soliton velocity approaches the speed of sound β_s from below; the amplitude of the acoustic pulse goes to infinity when the soliton velocity approaches the critical velocity $\beta_{\rm cr}$ from above. Physically, at slightly above the critical velocity, linearization of the refractive index against the material density will not be a valid approximation, and physical GASs will not exist in that range without modification.

Figure 2 shows a quiescent GAS with a soliton parameter $Q=\pi/2$, material properties typical of fused silica, and a wavelength of 0.8 μm. Figure 3 shows a similar GAS, but with velocity ten times the speed of sound. Figure 4 shows a GAS with velocity equal to half the group velocity of light in the medium.

Note that there are no purely optical solitons without an acoustic component; purely acoustic pulses are possible. In the case of zero phonon viscosity $\Gamma=0$, these have the form $u=v=0$, while the phonon field w is a combination of two arbitrary functions, $w(z,t)=w_+(z-\beta_s t)$ and $w_-(z+\beta_s t)$, which represent forward- and backward-moving acoustic waves.

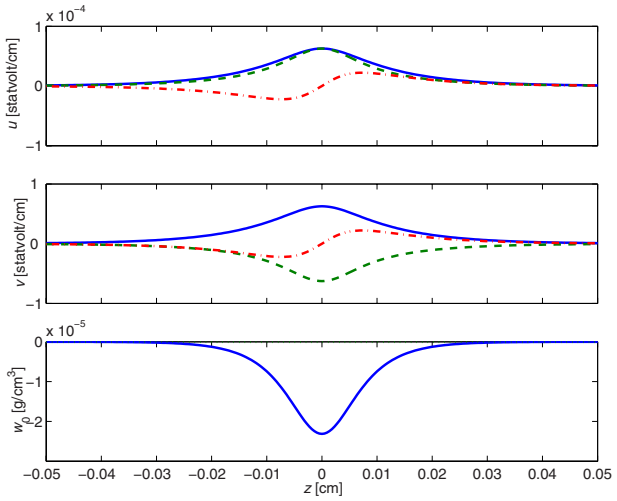

Fig. 3. (Color online) GAS with velocity ten times the speed of sound $\beta=10\beta_s=59$ km/s, and frequency in the middle of the bandgap, $Q=\pi/2$. The physical parameters are typical of bulk fused silica, and the Bragg coefficient is $\kappa=90\ {\rm cm}^{-1}$. The first part of the figure shows the amplitude of the envelope u of the forward-moving electromagnetic wave, the middle part shows the envelope v of the backward-moving wave, and the bottom part shows the acoustic field (material density). Solid lines are for the magnitudes of the amplitudes, dashed lines for the real parts, and dotted lines are for the imaginary parts.

5. GAS ENERGY, MOMENTUM, PHOTONS, AND MASS

A lot of physics can be inferred from the conserved (or quasi-conserved for finite Γ) quantities M,N,P,H for a GAS. The soliton's mass, photon energy (or number of

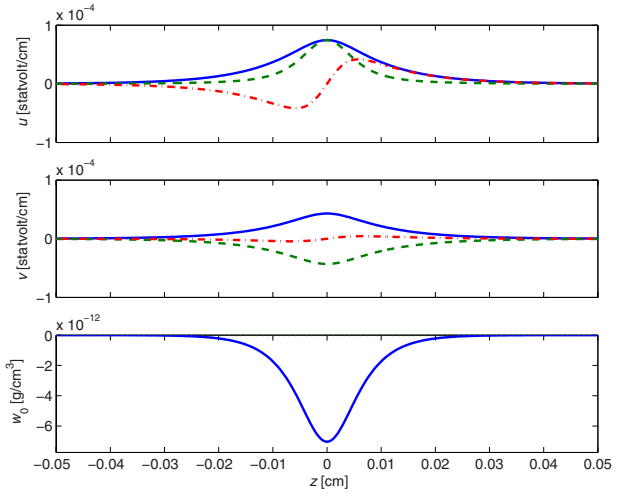

Fig. 4. (Color online) GAS with velocity half the group velocity of light in the medium $\beta=0.5/k_0'=1.03\times10^8$ m/s, and frequency in the middle of the bandgap, $Q=\pi/2$. The physical parameters are typical of bulk fused silica, and the Bragg coefficient is $\kappa=90\ {\rm cm}^{-1}$. The top part of the figure shows the amplitude of the envelope u of the forward-moving electromagnetic wave, the middle part shows the envelope v of the backward-moving wave, and the bottom part shows the acoustic field (material density).

photons), momentum, and energy are obtained by substituting the soliton formulas (9) and (10) into Eqs. (8) to obtain

$$M_{\mathrm{GAS}} = \frac{\lambda_{es}}{\beta_s^2 - \beta^2} A 4|\alpha|^2 Q, \tag{12a}$$

$$N_{\mathrm{GAS}} = \frac{n(\omega_0)^2}{4\pi} A 4|\alpha|^2 Q, \tag{12b}$$

$$P_{\mathrm{GAS}} = \frac{n(\omega_0)^2}{4\pi\omega_0} A(\beta k_0')\gamma|\kappa|(4|\alpha|^2)\Bigg[\sin Q + (4|\alpha|^2)\gamma^2\left(\frac{2\pi(\omega_0/c)^2}{k_0}\chi_s + \frac{\lambda_{es}\chi_{es}}{\beta_s^2 - \beta^2}\right)(\sin Q - Q\cos Q) + (4|\alpha|^2)\frac{\lambda_{es}\chi_{es}/(k_0')^2}{(\beta_s^2 - \beta^2)^2}(\sin Q - Q\cos Q)\Bigg], \tag{12c}$$

$$H_{\mathrm{GAS}} = \frac{n(\omega_0)^2/k_0'}{4\pi\omega_0} A\gamma|\kappa|(4|\alpha|^2)\Bigg\{\sin Q + \gamma^{-2}(\sin Q - Q\cos Q) - |\alpha|^2\frac{2\pi(\omega_0/c)^2}{k_0}\{\chi_s\gamma^2[1 - 4(\beta k_0')^2 - (\beta k_0')^4] + \chi_x\gamma^{-2}\} \times(\sin Q - Q\cos Q) + |\alpha|^2\frac{\chi_{es}\lambda_{es}}{\beta_s^2 - \beta^2}\Bigg[\frac{-2\beta_s^2 + 6\beta^2}{\beta_s^2 - \beta^2} + 4(\beta k_0')^2\gamma^2\Bigg](\sin Q - Q\cos Q)\Bigg\}. \tag{12d}$$

Recall that A is the area of the transverse modes of the fields in the waveguide; set it to unity for M, N, P, H per unit area. There is an implicit dependence on the GAS velocity β via the GAS amplitude factor α. Note that the dependence on the parameter Q is quite simple. In Eq. (12c) for the soliton momentum, the first two terms on the right hand side are the momentum carried by light, and the third term is the momentum in the acoustic field.

Figures 5–8 show the conserved quantities over the full range of soliton velocities β for a specific soliton parameter $Q=\pi/2$, for which the solitons are in the middle of the bandgap. The coefficients are those of bulk fused silica, as detailed in Section 2. Each of Figs. 5–8 shows what the dependence on velocity would be without electrostriction (dependence of the refractive index n on the density w) and then the conserved quantities for the solitons using the physically correct (nonzero) $\partial n/\partial W$. The dependence of the conserved quantities on Q is much simpler than the dependence on β, with different values of Q generally making for moderate quantitative but not qualitative differences in the plots versus soliton velocity. The mass M and photon energy (or number of photons) N increase linearly with the soliton parameter Q; the momentum P and Hamiltonian H are the sum of two functions of β, each multiplied by either $\sin Q$ or $(\sin Q - Q\cos Q)$. Figures 5 and 6 plot the mass and number of photons (per cross-sectional area) in bulk silica. The photon energy per

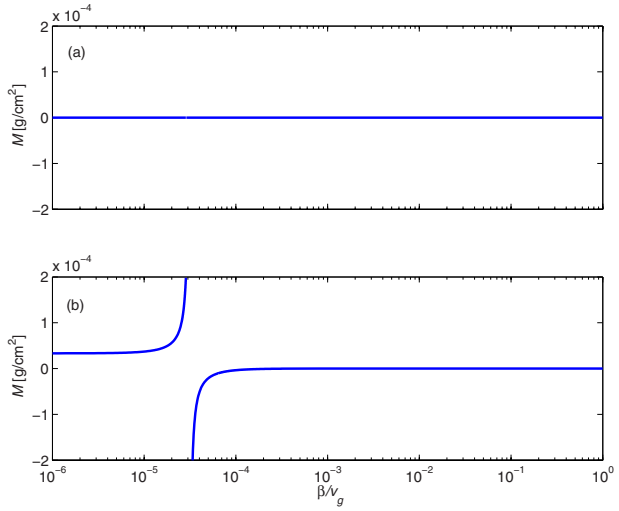

Fig. 5. (Color online) Mass, or integrated material density variation, per cross-sectional area (M) of GASs in bulk silica with physical parameters as given in the text. The velocities (β) range from zero up to the group velocity of light, and the frequencies are in the middle of the bandgap, $Q=\pi/2$. (a) shows what the mass would be, were there no dependence of the refractive index on the material density. (b) Soliton mass with physical values of the electrostrictive constants.

cross-sectional area N is positive definite, but the material mass M is positive for subsonic GASs and negative for supersonic GASs. Below the speed of sound $\beta<\beta_s$ $=5.9$ km/s, M, P, and H increase, while N decreases. The conserved quantities approach finite values as the soliton velocity approaches the speed of sound from below. Bright solitons do not exist between the speed of sound and the critical velocity $\beta_{\mathrm{cr}}=6.46$ km/s$=1.10\beta_s$. The conserved quantities are infinite at just above the critical velocity (i.e., as the soliton approaches the critical velocity from above). Above the critical velocity ($\beta>\beta_{\mathrm{cr}}$), the soliton mass M is negative, and it decreases in magnitude (in-

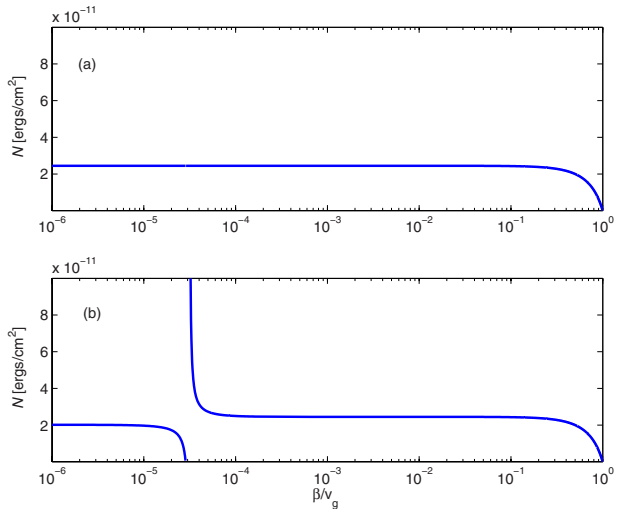

Fig. 6. (Color online) Photon energy (or number of photons) per cross-sectional area (N) of GASs in bulk silica at light wavelength of 0.8 μm. The velocities (β) range from zero up to the group velocity of light, and the frequencies are in the middle of the bandgap, $Q=\pi/2$. (a) Photon energy N, if there were no dependence of the refractive index on the material density. (b) The soliton's photon energy N, with $\partial n/\partial W=0.2$ cm^3/g.

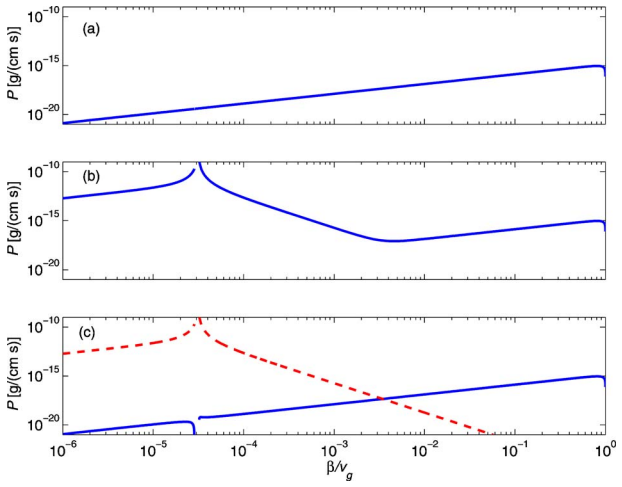

Fig. 7. (Color online) Momentum per cross-sectional area (P) of GASs in bulk silica at wavelength of 0.8 μm. The velocities (β) range from zero up to the group velocity of light, and the frequencies are in the middle of the bandgap, $Q=\pi/2$. (a) Momentum, if there were there no dependence of the refractive index on the material density. (b) Soliton momentum with physical values of the electrostrictive constants. (c) Momentum in the light (solid line) and sound (dashed line) separately.

creases in value) as a function of velocity. Above the critical velocity, the photon energy (also called the number of photons) N in the soliton decreases with velocity. The momentum of supersonic GASs first decreases with velocities above the critical velocity due to the change in mass of the soliton. Then, near $\beta=9.34\times10^5$ m/s$=158\beta_s=v_g/221$, the momentum increases, when the momentum in the photons is more than the momentum in the phonons. At even higher velocities, $\beta=1.68\times10^9$ m/s $=0.81v_g$, the momentum decreases again because the positive self-phase modulation decreases the intensity of the GAS. The Hamiltonian of supersonic GASs first decreases quickly, then flattens out, and at close to the group velocity there is a moderate increase and then a sharp drop.

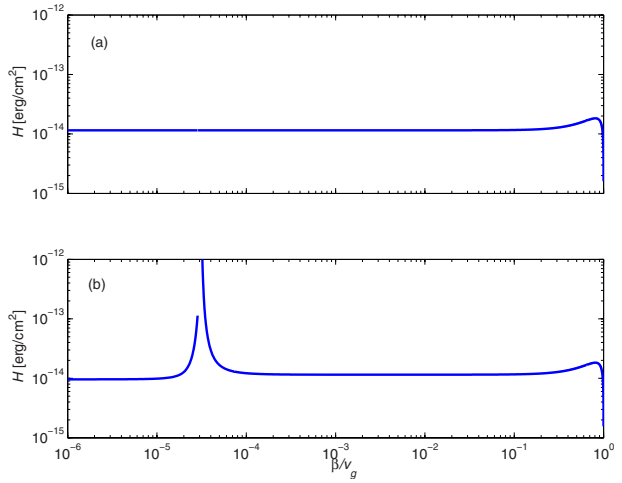

Fig. 8. (Color online) Hamiltonian per cross-sectional area (H) of GASs in bulk silica with the typical physical parameters as given in the text. The velocities (β) range from zero up to the group velocity of light, and the frequencies are in the middle of the bandgap, $Q=\pi/2$. (a) Hamiltonian, if there were no dependence of the refractive index on the material density. (b) The soliton's Hamiltonian energy with nonzero values of the electrostrictive constants, χ_{es} and λ_{es}.

6. SUDDEN ACCELERATION AND DECELERATION

Some predictions about GAS dynamics can be made based on the quasi-conserved quantities, given in Eqs. (8) and illustrated in Figs. 5–8. The momentum P_{GAS} is especially critical. If a soliton experiences a supersonic instability—the instability of the GAS when the velocity is larger than the speed of sound (see [20])—the system following the instability cannot have more Hamiltonian, momentum, or photon energy than the original soliton. Because some of the faster-moving solitons have less momentum than the slower-moving solitons (and not significantly less Hamiltonian either), a slow-moving soliton may decay into a fast-moving soliton. And if a fast-moving soliton experiences an instability, the large momenta contained in slow but non-quiescent solitons may keep the soliton from decaying by slowing down to anything more than velocity at virtually zero.

The supersonic instability leading to the abrupt acceleration of a GAS can be seen in Figs. 9–12. Both simulations assume that the medium is fused silica, with a central wavelength of 0.8 μm, and a Bragg scattering coefficient of $\kappa=90$/cm (which is relatively large, making the GASs shorter and more intense). The first simulation is for a GAS with $Q=\pi/3$ and an initial velocity ten times the speed of sound, $\beta=10\beta_s$. The instability takes hold, and the result is a GAS with the same Q and velocity $\beta=1.2\times10^7$ m/s$=1600\beta_s=0.046v_g$. A density variation is left behind when the new fast-moving GAS runs away. You can also observe high-frequency acoustic waves w_u, w_v developing initially before the GAS accelerates, then getting left behind, and also visible is a tail (or wake) of high-frequency acoustic waves following the fast-moving soliton. In the second simulation displayed, the initial conditions are the same, except that the Q-value of the

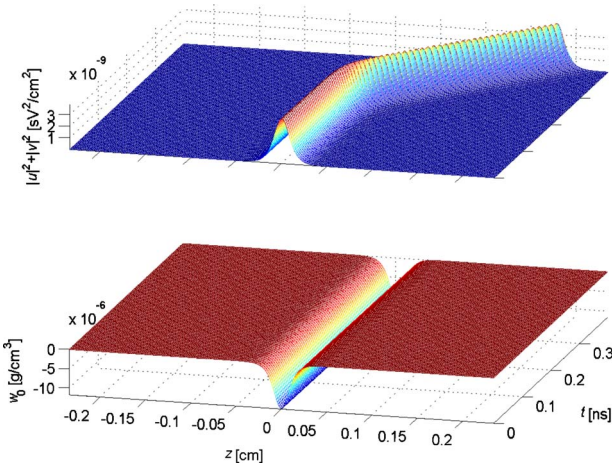

Fig. 9. (Color online) GAS in fused silica with initial velocity ten times the speed of sound, $\beta=10\beta_s$, and $Q=\pi/3$. Following realization of the supersonic instability, a much faster GAS ($\beta=1600\beta_s$) is produced, and a slowly decaying density variation remains behind.

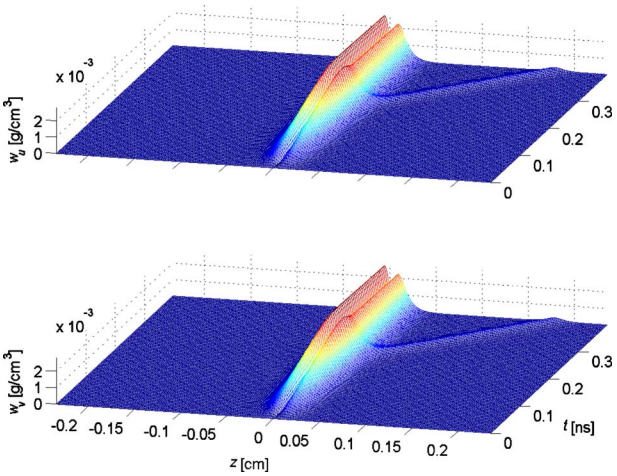

Fig. 10. (Color online) High-frequency acoustic (Brillouin) waves interacting with light in the run depicted in Fig. 9. The Brillouin waves are initially zero and grow due to excitation by the light. When the GAS suddenly speeds up, some Brillouin waves are left behind, and the now faster-moving soliton produces its own wake.

initial GAS is $\pi/2$. After the instability, some light is emitted left and right to dispersive (non-soliton) radiation, and the remaining light reforms a GAS with $Q=0.25\pi$ and Q, and velocity $\beta=1.2\times10^7$ m/s$=2000\beta_s=0.058v_g$.

The supersonic instability leading to the sudden deceleration of a GAS to zero velocity can be seen in Figs. 13 and 14. As above, the medium is fused silica, the central wavelength is 0.8 μm, and the Bragg coefficient is $\kappa=90$/cm. The initial soliton has $Q=\pi/3$ and velocity $\beta=6.9\times10^5$ m/s$=v_g/300=117\beta_s$. The instability takes hold and stops the soliton. There are 5 orders of magnitude between the speed of sound and the speed of light, so the light oscillates many times within the interaction region while the low wave number acoustic wave develops and expands outward relatively slowly. The high wave number (Brillouin) phonons (w_u,w_v) also develop, but play a very minor role in this instance.

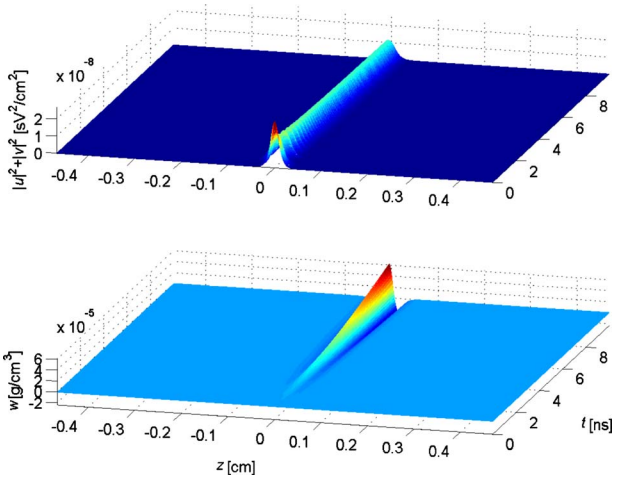

Fig. 11. (Color online) GAS in fused silica with initial velocity ten times the speed of sound, $\beta=10\beta_s$, and $Q=\pi/2$. After the supersonic instability, about half of the light escapes as a dispersive (non-soliton) radiation, and the remaining light reforms a much faster GAS (velocity $\beta=2000\beta_s$) with $Q=0.25\pi$. A slowly decaying low-frequency density variation is left behind.

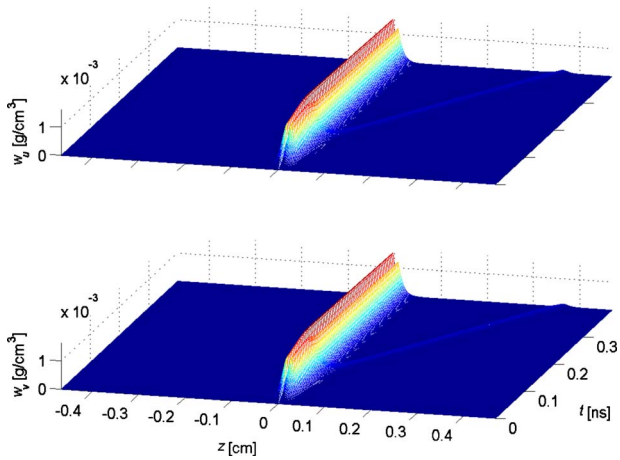

Fig. 12. (Color online) The high-frequency acoustic (Brillouin) waves interacting with the light in the run depicted in Fig. 11. As in the prior simulation, the Brillouin waves are initially zero and grow due to excitation by the light. When the GAS suddenly speeds up, some Brillouin waves are left behind, and the now faster-moving soliton produces its own wake.

7. CONCLUSIONS

We derived a set of propagation equations to describe light in a nonlinear fiber with a Bragg grating, coupled by electrostriction to low-frequency (sound) and high-frequency (ultrasonic) acoustic waves. Forward- and backward-moving light in the vicinity of the bandgap can interact with acoustic waves of low wave numbers—in which case the interaction is generally referred to as electrostriction—or high wave numbers, twice the wave number of light—in which case the interaction is called Brillouin scattering.

There is a localized structure in this system, a gap-acoustic soliton (GAS), for the case when Brillouin scattering may be neglected and when phonon viscosity is zero. GASs exist in the same bandgap as standard gap

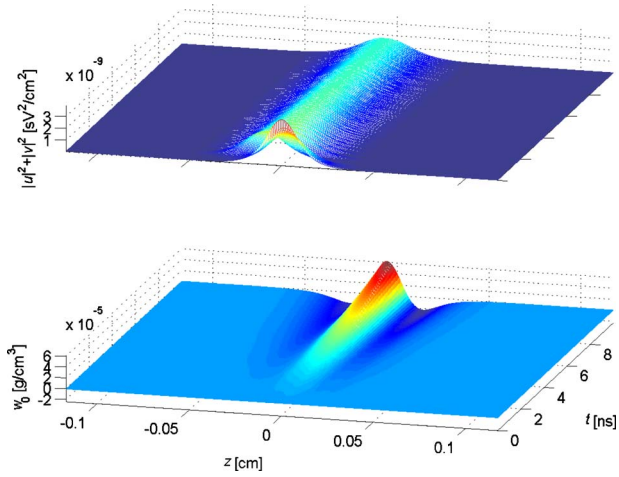

Fig. 13. (Color online) GAS in fused silica with initial velocity of $\beta=6.9\times10^5$ m/s$=v_g/300$ and $Q=\pi/3$. Following realization of the supersonic instability, the GAS comes to a stop while emitting acoustic waves to the left and to the right.

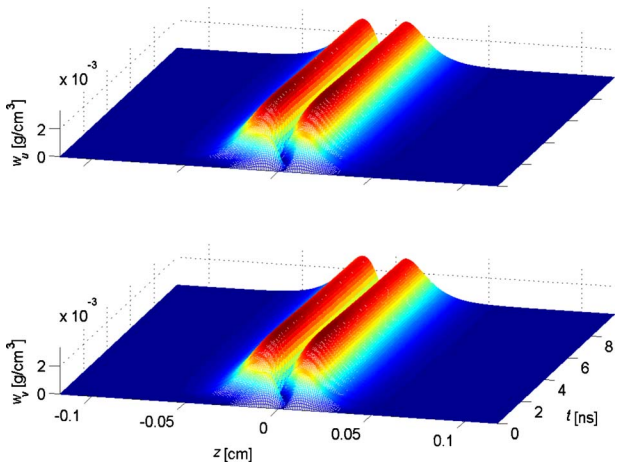

Fig. 14. (Color online) High-frequency acoustic (Brillouin) waves interacting with light in the run depicted in Fig. 13.

solitons (without electrostriction). GASs exist at velocities from zero up to the group velocity of light in the medium, except for a velocity gap from the speed of sound, just below which the phonon component of the GAS approaches zero, up to a critical velocity (which is about 10% higher than the speed of sound for the case of fused silica), just above which the acoustic component of the GAS is asymptotically large.

Electrostriction introduces a "supersonic" instability for GASs moving faster than the speed of sound [20]. In most cases, the result of the supersonic instability was the re-formation of a new GAS at a different velocity. By analyzing the GASs' conserved quantities—especially the momentum, which due to the acoustic parts of the soliton is much higher at many low velocities than at many high velocities. We predicted that the post-instability GASs may in some cases have velocities much higher than that of the original soliton. In other cases, the resulting soliton may have velocity almost equal to zero. These predictions of the abrupt acceleration and drastic deceleration are confirmed by a direct numerical simulation of the system.

For a waveguide of fused silica (i.e., glass), the momentum and acoustic effects dominate the solitons' behavior when the velocity is less than approximately 0.5% of the group velocity of light. The usual gap soliton model, in which the dependence of the refractive index on the material density is neglected, may be accurate when the solitons are moving at more than 1% of the speed of light, but at slower velocities the GAS model is essential.

APPENDIX A: PROPAGATION EQUATIONS FOR LIGHT AND SOUND

Light propagation is governed by the Maxwell's equations, and sound propagation in glass can be described by the wave equation with a viscosity term. Light and sound interact via electrostriction. For optical gap solitons, light is centered at one frequency, but the direction can be either forward or backward; the electromagnetic field's dynamics can then be described by two separate equations: one for the forward-moving light and one for the backward-moving light. The acoustic fields that interact with this light can be of high or low wave number. The high wave number acoustic fields can be either forward- or backward-moving. The low wave number acoustic field is centered at wave number zero. The acoustic field for this system can then be broken down into three equations: two for the high wave number phonons and one for the low wave number phonons.

1. Electromagnetic Field Equations with Phonon Perturbations

Starting from the Maxwell's equations, we can consider an isotropic medium without free charges, currents, or magnetic polarization. Bragg and Brillouin scattering from acoustic waves will be included as extensions of this. The electromagnetic field and the linear and nonlinear polarization of the medium obey

$$\nabla \cdot (\mathbf{E} + 4\pi \mathbf{P}_{\text{linear}} + 4\pi \mathbf{P}_{\text{NL}}) = 0, \tag{A1a}$$

$$\nabla \cdot \mathbf{B} = 0, \tag{A1b}$$

$$\nabla \times \mathbf{E} = -\frac{1}{c}\frac{\partial}{\partial t}\mathbf{B}, \tag{A1c}$$

$$\nabla \times \mathbf{B} = -\frac{1}{c}\frac{\partial}{\partial t}(\mathbf{E} + 4\pi \mathbf{P}_{\text{linear}} + 4\pi \mathbf{P}_{\text{NL}}). \tag{A1d}$$

The dependence of polarization $\mathbf{P}=\mathbf{P}_{\text{linear}}+\mathbf{P}_{\text{NL}}$ on the electromagnetic field $\mathbf{E},\mathbf{B}$ is taken to have a part which is linear in the electromagnetic field, with an additional dependence on the density of the material,

$$\mathbf{E} + 4\pi \mathbf{P}_{\text{linear}} \equiv \mathbf{D} = n^2(\omega, w)\mathbf{E}, \tag{A2a}$$

where the expression on the right hand side, relating the electric displacement to electric field via a frequency-dependent index of refraction, holds in the frequency space as well as in real space for monochromatic fields. We have indicated a dependence of the refractive index n on the density of the material w. Part of the polarization arises from a third-order Kerr nonlinearity,

$$\mathbf{P}_{\text{NL}} = \chi^{(3)}(\mathbf{E} \cdot \mathbf{E})\mathbf{E}. \tag{A2b}$$

Fourier transforming the time dimension to the frequency space, and assuming isotropy, Coulomb's [Eq. (A1a)] and Ampere's [Eq. (A1d)] laws are

$$0 = n^2(\omega)\, \nabla \cdot \mathbf{E}(\mathbf{x}, \omega) + 4\pi \nabla \cdot \mathbf{P}_{\text{NL}}(\mathbf{x}, \omega), \tag{A3a}$$

$$0 = \nabla \times \mathbf{B}(\mathbf{x}, \omega) + i\frac{\omega}{c}[n^2(\omega)\mathbf{E}(\mathbf{x}, \omega) + 4\pi \mathbf{P}_{\text{NL}}(\mathbf{x}, \omega)]. \tag{A3b}$$

Taking the curl of both sides of Faraday's law [Eq. (A1c)], and inserting the above expressions, gives—after some algebraic manipulation—the wave equation,

$$0 = \left[\nabla^2 + \frac{n^2(\omega)\omega^2}{c^2}\right]\mathbf{E}(\mathbf{x},\omega) + \frac{4\pi\omega^2}{c^2}\mathbf{P}_{\mathrm{NL}}(\mathbf{x},\omega) + \frac{4\pi}{n^2(\omega)}\nabla[\nabla\cdot\mathbf{P}_{\mathrm{NL}}(\mathbf{x},\omega)]. \quad \text{(A4a)}$$

A Fourier transform in the spatial dimensions gives the wave equation in momentum space,

$$0 = \left[k^2 - \frac{n^2(\omega)\omega^2}{c^2}\right]\mathbf{E}(\mathbf{k},\omega) - \frac{4\pi\omega^2}{c^2}\left\{\mathbf{P}_{\mathrm{NL}}(\mathbf{k},\omega) - \frac{c^2}{n^2(\omega)\omega^2}\mathbf{k}[\mathbf{k}\cdot\mathbf{P}_{\mathrm{NL}}(\mathbf{k},\omega)]\right\}. \quad \text{(A4b)}$$

If the nonlinear polarization is transverse, which is the case for the Kerr nonlinearity (A2b), and the electric field is transverse, the last terms on the right-hand sides of Eqs. (A4) vanish. The basic optical gap soliton has one (nontrivial) spatial dimension, and for light of one polarization, we reduce the mathematical model to

$$0 = \left[\frac{\partial^2}{\partial z^2} + \frac{n^2(\omega)\omega^2}{c^2}\right]E(z,\omega) + \frac{4\pi\omega^2}{c^2}P_{\mathrm{NL}}(z,\omega), \quad \text{(A5a)}$$

or, equivalently,

$$0 = \left[k^2 - \frac{n^2(\omega)\omega^2}{c^2}\right]E(k,\omega) - \frac{4\pi\omega^2}{c^2}P_{\mathrm{NL}}(k,\omega). \quad \text{(A5b)}$$

Considering the wave equations (A5) in the vicinity of frequency ω_0 and wave number k_0, completing the square for the quadratic equation, Taylor expanding in the small terms, and truncating we find

$$0 = \left[(k_0+\delta k)^2 - \frac{n^2(\omega_0+\delta\omega)(\omega_0+\delta\omega)^2}{c^2} - \frac{4\pi(\omega_0+\delta\omega)^2}{c^2}\frac{P_{\mathrm{NL}}(k_0+\delta k,\omega_0+\delta\omega)}{E(k_0+\delta k,\omega_0+\delta\omega)}\right]E(k_0+\delta k,\omega_0+\delta\omega), \quad \text{(A6a)}$$

$$0 = \left[\mp(k_0+\delta k) + \frac{n(\omega_0+\omega)(\omega_0+\omega)}{c}\sqrt{1+\frac{4\pi}{[n(\omega_0+\omega)]^2}\frac{P_{\mathrm{NL}}}{E}}\right]E(k_0+\delta k,\omega_0+\delta\omega) \quad \text{(A6b)}$$

$$= \mp(k_0+\delta k)E(k_0+\delta k,\omega_0+\delta\omega) + \frac{n(\omega_0+\omega)(\omega_0+\omega)}{c}E + \frac{2\pi(\omega_0+\omega)}{n(\omega_0+\omega)c}P_{\mathrm{NL}}(k_0+\delta k,\omega_0+\delta\omega)+\cdots \quad \text{(A6c)}$$

$$= \mp\delta kE(k_0+\delta k,\omega_0+\delta\omega) + \left(\frac{n(\omega_0)\omega_0}{c}\mp k_0\right)E + \frac{\partial}{\partial\omega}\left(\frac{n(\omega)\omega}{c}\right)_{\omega_0}\omega E + \frac{2\pi\omega_0/c}{n(\omega_0)}P_{\mathrm{NL}}(k_0+\delta k,\omega_0+\delta\omega)+\cdots. \quad \text{(A6d)}$$

Now, Fourier transforming back to real space, and including a non-uniformity in the index of refraction, partly fixed [i.e., arising from $\Delta n(z)$] and partly as a function of the material density [i.e., arising from $(\partial/\partial W)n(z,t)$], we obtain

$$0 = ik_0'\frac{\partial}{\partial t}E(z,t) \pm i\frac{\partial}{\partial z}E + \left(\frac{n(\omega_0,z,W)\omega_0}{c}\mp k_0\right)E + \frac{2\pi(\omega_0/c)^2}{k_0}P_{\mathrm{NL}}(z,t)+\cdots \quad \text{(A7a)}$$

$$= ik_0'\frac{\partial}{\partial t}E(z,t) \pm i\frac{\partial}{\partial z}E + \left(\frac{\omega_0}{c}\Delta n(z) + \frac{\omega_0}{c}\frac{\partial n}{\partial W}W\right)E + \frac{2\pi(\omega_0/c)^2}{k_0}P_{\mathrm{NL}}(z,t)+\cdots, \quad \text{(A7b)}$$

where $k_0 = \pm n(\omega_0)\omega_0/c$ is the phase velocity and $k_0' = (d/d\omega)[n(\omega)\omega/c]_{\omega=\omega_0}$ is the reciprocal of the group velocity (v_g). Where arguments of the index of refraction are not given explicitly, they are based on an average value at a baseline material density W. The result will be an equation for a SVE about a carrier wave with wave vector (k_0,ω_0).

Equations (A7) apply to any quasi-monochromatic electromagnetic field with any nonlinearity. For the optical gap soliton, there is one frequency of light in the system, and light may be traveling forward or backward. The electric field E may then be written as two SVEs about carrier waves with frequencies $\omega=\omega_0$ and wave numbers $k=\pm k_0 = \pm n(\omega_0)\omega_0/c$. The acoustic fields that may interact with these light fields are those centered at wave numbers $k=0$ and $\pm 2k_0$. If the speed of sound, which we refer to as β_s, is constant, then the frequencies of the acoustic waves are simply the speed of sound (β_s) times the wave numbers. We also allow the index of refraction to have a small component at half the wavelength of light, which will act as a Bragg scatterer,

$$E(z,t) = u(z,t)\exp[i(k_0z-\omega_0t)] + v(z,t)\exp[-i(k_0z+\omega_0t)] + u(z,t)^*\exp[-i(k_0z-\omega_0t)] + v(z,t)^*\exp[i(k_0z+\omega_0t)], \quad \text{(A8a)}$$

$$W(z,t) = w_u(z,t)\exp[2ik_0(z-\beta_st)] + w_v(z,t)\exp[-2ik_0(z+\beta_st)] + w_u(z,t)^*\exp[-2ik_0(z-\beta_st)] + w_v(z,t)^*\exp[2ik_0(z+\beta_st)] + w_0(z,t), \quad \text{(A8b)}$$

$$\Delta n(z) = \Delta n\cos(2k_0z). \quad \text{(A8c)}$$

Putting the fields in terms of SVEs [Eqs. (A8)] into the general dynamical equations for light [Eq. (A7b)], while

taking the nonlinearity to be Kerr [Eq. (A2b)], and separating the different frequency and wave number components gives

$$0 = ik_0' u_t + iu_z + \kappa v + \frac{2\pi(\omega_0/c)^2}{k_0} 3\chi^{(3)}(|u|^2 + 2|v|^2)u + \chi_{es}[w_0 u + \exp(-2ik_0\beta_s t)w_u v + \exp(2ik_0\beta_s t)w_v^* v], \tag{A9a}$$

$$0 = ik_0' v_t - iv_z + \kappa^* u + \frac{2\pi(\omega_0/c)^2}{k_0} 3\chi^{(3)}(2|u|^2 + |v|^2)v + \chi_{es}[w_0 v + \exp(2ik_0\beta_s t)w_u^* u + \exp(-2ik_0\beta_s t)w_v u], \tag{A9b}$$

where

$$\kappa \equiv \frac{\omega_0}{c}\frac{\Delta n}{2}, \quad \chi_{es} \equiv \frac{\omega_0}{c}\frac{\partial n}{\partial W}. \tag{A10}$$

This assumes that the speed of sound β_s is small enough so that the frequencies $2k_0\beta_s$ are within the frequency spread of the SVEs u and v. These are the equations for the dynamics of the SVEs of light.

2. Acoustic Wave Equations with Electrostrictive Perturbations

To complete the dynamical system, we need equations for the dynamics of the density of the material, i.e., acoustic waves. In silica glass, the speed of sound has a very weak dependence on the wave number or frequency, and acoustic waves are also subject to viscosity [32]. The dependence of the index of refraction on the density of the material creates electrostriction, a force (pressure gradient) attracting the material to regions of a higher light intensity. The evolution equation for the density is [27,53]

$$0 = \frac{\partial^2}{\partial t^2} W(\mathbf{x},t) - \beta_s^2 \nabla^2 W - \Gamma \frac{\partial}{\partial t}\nabla^2 W + \frac{\lambda_{es}}{2}\nabla^2 \langle E(\mathbf{x},t)^2\rangle, \tag{A11}$$

where $W(\mathbf{x},t)$ is the density of the material, $E(\mathbf{x},t)$ is the amplitude of the electric field, $\nabla^2 = \partial^2/\partial x^2 + \partial^2/\partial y^2 + \partial^2/\partial z^2$ is the Laplacian, β_s is the speed of sound, Γ is a phonon viscosity coefficient, and λ_{es} is an electrostrictive coefficient. We will focus on single-mode waveguides, in which any transverse dynamics are trivial. This reduces the system to 1+1-dimensions,

$$0 = \frac{\partial^2}{\partial t^2} W(z,t) - \beta_s^2 \frac{\partial^2}{\partial z^2} W - \Gamma \frac{\partial^3}{\partial t\, \partial z^2} W + \frac{\lambda_{es}}{2}\frac{\partial^2}{\partial z^2}\langle E(z,t)^2\rangle. \tag{A12}$$

Since we will be dealing with optical gap solitons, light in the system is approximately monochromatic and may be moving forward or backward, as expressed by Eq. (A8a). Electrostrictive response times are on the order of 10^{-9} s [27]. This is several (~6) orders of magnitude slower than the temporally fast-varying terms ($\propto u^2, v^2, u^{*2}, v^{*2}$) for visible or near infrared light, so these may be dropped from the averaged square field in the phonon equation (A12),

$$0 = W_{tt} - \beta_s^2 W_{zz} - \Gamma W_{tzz} + \lambda_{es}[|u|^2 + |v|^2 + uv^* \exp(2ik_0 z) + u^* v \exp(-2ik_0 z)]_{zz}, \tag{A13}$$

where subscripts denote partial derivatives. Since $u(z,t)$ and $v(z,t)$ are SVEs, the phonons' source terms will be centered at wave numbers $k=0$, $2k_0$, and $-2k_0$. Thus light in the optical gap solitons will interact by electrostriction only with phonons around those same wave numbers, consistent with Eq. (A8b). The Fourier transform of the phonon equation (A13) to the momentum-frequency space is

$$0 = -\omega^2 W(k,\omega) - i\omega k^2 \Gamma W + k^2\beta_s^2 W - k^2\lambda_{es}\mathcal{F}\{|u|^2 + |v|^2\}(k,\omega) - k^2\lambda_{es}\mathcal{F}\{uv^*\}(k-2k_0,\omega) - k^2\lambda_{es}\mathcal{F}\{u^*v\}(k+2k_0,\omega). \tag{A14}$$

Since u and v are SVEs, $\mathcal{F}\{|u|^2+|v|^2\}(k,\omega)$ will only be significant in the vicinity of $k\approx 0$, $\mathcal{F}\{uv^*\}(k-2k_0,\omega)$ will only be significant at $k\approx 2k_0$, and $\mathcal{F}\{u^*v\}(k+2k_0,\omega)$ will only be significant at $k\approx -2k_0$. Substituting the sum of SVEs [Eq. (A8b)] into the general phonon equation (A14), and separating into the different (and, in the k-space, nonoverlapping) regions,

$$0 = -\omega^2 w_0(k,\omega) - i\omega k^2\Gamma w_0 + k^2\beta_s^2 w_0 - k^2\lambda_{es}\mathcal{F}\{|u|^2+|v|^2\} \times(k,\omega), \tag{A15a}$$

$$0 = (\omega-\omega_0)^2 w_u(k,\omega) + i\Gamma(\omega-\omega_0)(k-2k_0)^2 w_u - (k-2k_0)^2\beta_s^2 w_u + (k-2k_0)^2\lambda_{es}\mathcal{F}\{uv^*\}(k-2k_0,\omega-\omega_0), \tag{A15b}$$

$$0 = (\omega-\omega_0)^2 w_v(k,\omega) + i\Gamma(\omega-\omega_0)(k+2k_0)^2 w_v - (k+2k_0)^2\beta_s^2 w_v + (k+2k_0)^2\lambda_{es}\mathcal{F}\{u^*v\}(k+2k_0,\omega-\omega_0). \tag{A15c}$$

Here $w_u(k,\omega) = W(k-2k_0,\omega-\omega_0)$, $w_v(k,\omega) = W(k+2k_0,\omega-\omega_0)$, and $w_0(k,\omega) = W(k,\omega)$ are SVEs (in contrast to W, which is not a SVE).

a. Slowly Varying Phonon Field

Taking the phonon equation (A15a), which is for the region near the (k,ω) origin, or the slowly varying part of the phonon field, and inverse Fourier transforming it to real space, we obtain

$$0 = w_{0,tt} - \beta_s^2 w_{0,zz} - \Gamma w_{0,tzz} + \lambda_{es}(|u|^2 + |v|^2)_{zz}. \tag{A16}$$

This is the most useful form of the governing equations for low wave number (long-wavelength) acoustic waves.

b. Brillouin Scattering—High-Frequency Phonons

Now consider Eq. (A15b), the dynamics of the part of the phonon field with wave numbers close to $k=2k_0$. Complete the square, expand the root into a Taylor series, assuming that the nonlinear term is smaller than the linear terms, and drop higher-order terms to obtain

$$0 = [\omega + 2i(k_0 + k/2)^2\Gamma + \omega_u \pm 2(k_0 + k/2)\beta_s\{1 - (1/2)[(k_0 + k/2)\Gamma/\beta_s]^2\}]w_u(k,\omega) \mp (k_0 + k/2)\lambda_{es}\beta_s^{-1}\mathcal{F}\{uv^*\}(k,\omega + \omega_0) + \cdots. \quad \text{(A17)}$$

Choosing $\omega_0 = 2k_0\beta_s[1-(1/2)(k_0\Gamma/\beta_s)^2]$, and dropping the wave-number-dependence of the damping, higher-order dispersion, and a self-steepening-like term, we obtain

$$0 = \{\omega + 2ik_0^2\Gamma \pm k\beta_s[1 - (3/2)\times(k_0\Gamma/\beta_s)^2]\}w_u(k,\omega) \mp k_0\lambda_{es}\beta_s^{-1}\mathcal{F}\{uv^*\}(k,\omega \mp 2k_0\beta_s[1 - (1/2)(k_0\Gamma/\beta_s)^2]) + \cdots. \quad \text{(A18)}$$

Inverse Fourier transforming this to real space,

$$0 = iw_{u,t} + i(2k_0^2\Gamma)w_u \mp i\beta_s[1 - (3/2)\times(k_0\Gamma/\beta_s)^2]w_{u,z} \mp \frac{k_0\lambda_{es}}{\beta_s}\exp\{\mp 2ik_0\beta_s[1 - (1/2)\times(k_0\Gamma/\beta_s)^2]t\}(uv^*) + \cdots. \quad \text{(A19)}$$

The positive sign corresponds to the equality for the field w_u. The phonon viscosity is generally a small perturbation, so drop terms that are quadratic or higher in it,

$$0 = iw_{u,t} + i\beta_s w_{u,z} + i(2k_0^2\Gamma)w_u + \frac{k_0\lambda_{es}}{\beta_s}\exp(2ik_0\beta_s t)uv^*. \quad \text{(A20a)}$$

The corresponding equation for the Brillouin field moving in the opposite direction ($k = -2k_0$) is

$$0 = iw_{v,t} - \beta_s w_{v,z} + i(2k_0^2\Gamma)w_v + \frac{k_0\lambda_{es}}{\beta_s}\exp(2ik_0\beta_s t)uv^*. \quad \text{(A20b)}$$

3. The Bragg–Brillouin–Kerr System

Collecting the definitions of the SVEs of the electromagnetic and phonon fields,

$$E(z,t) = u(z,t)\exp[i(k_0 z - \omega_0 t)] + v(z,t)\exp[-i(k_0 z + \omega_0 t)] + u(z,t)^*\exp[-i(k_0 z - \omega_0 t)] + v(z,t)^*\exp[i(k_0 z + \omega_0 t)], \quad \text{(A21a)}$$

$$W(z,t) = w_0(z,t) + w_u(z,t)\exp[2ik_0(z - \beta_s t)] + w_v(z,t)\exp[-2ik_0(z + \beta_s t)] + w_u(z,t)^*\exp[-2ik_0(z - \beta_s t)] + w_v(z,t)^*\exp[2ik_0(z + \beta_s t)], \quad \text{(A21b)}$$

we get the dynamical equations,

$$0 = ik_0' u_t + iu_z + \kappa v + \frac{2\pi(\omega_0/c)^2}{k_0}3\chi^{(3)}(|u|^2 + 2|v|^2)u + \chi_{es}[w_0 u + \exp(-2ik_0\beta_s t)w_u v + \exp(2ik_0\beta_s t)w_v^* v], \quad \text{(A22a)}$$

$$0 = ik_0' v_t - iv_z + \kappa u + \frac{2\pi(\omega_0/c)^2}{k_0}3\chi^{(3)}(2|u|^2 + |v|^2)v + \chi_{es}[w_0 v + \exp(2ik_0\beta_s t)w_u^* u + \exp(-2ik_0\beta_s t)w_v u], \quad \text{(A22b)}$$

$$0 = w_{0,tt} - \beta_s^2 w_{0,zz} - \Gamma w_{0,tzz} + \lambda_{es}(|u|^2 + |v|^2)_{zz}, \quad \text{(A22c)}$$

$$0 = iw_{u,t} + i\beta_s w_{u,z} + i(2k_0^2\Gamma)w_u + \frac{k_0\lambda_{es}}{\beta_s}\exp(2ik_0\beta_s t)uv^*, \quad \text{(A22d)}$$

$$0 = iw_{v,t} - i\beta_s w_{v,z} + i(2k_0^2\Gamma)w_v + \frac{k_0\lambda_{es}}{\beta_s}\exp(2ik_0\beta_s t)u^* v. \quad \text{(A22e)}$$

ACKNOWLEDGMENTS

This work was supported in part by grants from the U.S.–Israel Binational Science Foundation (grant no. 2006212), the Israel Science Foundation (ISF) (grant no. 29/07), and the James Franck German–Israel Binational Program in Laser–Matter Interactions.

REFERENCES

1. W. E. Thirring, "A soluble relativistic field theory," Ann. Phys. (N.Y.) **3**, 91–112 (1958).
2. E. A. Kuznetsov and A. V. Mikhailov, "On the complete integrability of the two-dimensional classical Thirring model," Theor. Math. Phys. **30**, 193–200 (1977).
3. D. J. Kaup and A. C. Newell, "On the Coleman correspondence and the soliton of the massive Thirring model," Lett. Nuovo Cimento **20**, 325–331 (1977).
4. B. J. Eggleton, C. Martijn de Sterke, and R. E. Slusher, "Bragg solitons in the nonlinear Schrödinger limit: experiment and theory," J. Opt. Soc. Am. B **16**, 587–599 (1999).
5. W. Chen and D. L. Mills, "Gap solitons and the nonlinear optical response of superlattices," Phys. Rev. Lett. **58**, 160–163 (1987).
6. D. N. Christodoulides and R. I. Joseph, "Slow Bragg solitons in nonlinear periodic structures," Phys. Rev. Lett. **62**, 1746–1749 (1989).
7. A. B. Aceves and S. Wabnitz, "Self-induced transparency solitons in nonlinear refractive periodic media," Phys. Lett. A **141**, 37–42 (1989).
8. J. T. Mok, C. M. de Sterke, I. C. M. Littler, and B. J. Eggleton, "Dispersionless slow light using gap solitons," Nat. Phys. **2**, 775–780 (2006).
9. M. D. Lukin and A. Imamoglu, "Controlling photons using electromagnetically induced transparency," Nature **413**, 273–276 (2001).
10. R. W. Boyd and D. J. Gauthier, "'Slow' and 'fast' light," Prog. Opt. **43**, 497–530 (2002).
11. M. S. Bigelow, N. N. Lepeshkin, and R. W. Boyd, "Superluminal and slow light propagation in a room-temperature solid," Science **301**, 200–202 (2003).
12. K. Y. Song, M. G. Herraez, and L. Thevenaz, "Observation of pulse delaying and advancement in optical fibers using stimulated Brillouin scattering," Opt. Express **13**, 82–88 (2005).
13. D. Dahan and G. Eisenstein, "Tunable all optical delay via slow and fast light propagation in a Raman assisted fiber optical parametric amplifier: a route to all optical buffering," Opt. Express **13**, 6234–6249 (2005).
14. Y. Zhang, W. Qui, J. Ye, N. Wang, J. Wang, H. Tian, and P. Yuan, "Controllable ultraslow light propagation in highly-doped erbium fiber," Opt. Commun. **281**, 2633–2637 (2008).
15. R. W. Boyd and D. J. Gauthier, "Controlling the velocity of light pulses," Science **326**, 1074–1077 (2009).
16. B. A. Malomed and R. S. Tasgal, "Vibration modes of a gap soliton in a nonlinear optical medium," Phys. Rev. E **49**,

5787–5796 (1994).
17. I. V. Barashenkov, D. E. Pelinovsky, and E. V. Zemlyanaya, "Vibrations and oscillatory instabilities of gap solitons," Phys. Rev. Lett. **80**, 5117–5120 (1998).
18. I. V. Barashenkov and E. V. Zemlyanaya, "Oscillatory instabilities of gap solitons: a numerical study," Comput. Phys. Commun. **126**, 22–27 (2000).
19. A. De Rossi, C. Conti, and S. Trillo, "Stability, multistability, and wobbling of optical gap solitons," Phys. Rev. Lett. **81**, 85–88 (1998).
20. R. S. Tasgal, Y. B. Band, and B. A. Malomed, "Optoacoustic solitons in Bragg gratings," Phys. Rev. Lett. **98**, 243902 (2007).
21. E. M. Dianov, A. V. Luchnikov, A. N. Pilipetskii, and A. N. Starodumov, "Electrostriction mechanism of soliton interaction in optical fibers," Opt. Lett. **15**, 314–316 (1990).
22. A. A. Zabolotskii, "Generation of pulses upon nonresonant acousto-electromagnetic interaction," Opt. Spectrosc. **97**, 936–944 (2004).
23. T. Iizuka and Y. S. Kivshar, "Optical gap solitons in nonresonant quadratic media," Phys. Rev. E **59**, 7148–7151 (1999).
24. S. V. Sazonov, "Optical-acoustic soliton under the conditions of slow light and stimulated Mandelstam–Brillouin scattering," JETP Lett. **81**, 201–204 (2005).
25. J. D. Jackson, *Classical Electrodynamics* (Wiley, 1975).
26. M. Born and E. Wolf, *Principles of Optics* (Pergamon, 1980).
27. R. W. Boyd, *Nonlinear Optics* (Academic, 2003).
28. G. P. Agrawal, *Nonlinear Fiber Optics* (Academic, 2006).
29. D. T. Hon, "Pulse compression by stimulated Brillouin scattering," Opt. Lett. **5**, 516–518 (1980).
30. I. Bongrand, C. Montes, E. Picholle, J. Botineau, A. Picozzi, G. Cheval, and D. Bahloul, "Soliton compression in Brillouin fiber lasers," Opt. Lett. **26**, 1475–1477 (2001).
31. P. Maák, G. Kurdi, A. Barócsi, K. Osvay, A. P. Kovács, L. Jakab, and P. Richter, "Shaping of ultrashort pulses using bulk acousto-optic filter," Appl. Phys. B **82**, 283–287 (2006).
32. E. Rat, M. Foret, G. Massiera, R. Vialla, M. Arai, R. Vacher, and E. Courtens, "Anharmonic versus relaxational sound damping in glasses. I. Brillouin scattering in densified silica," Phys. Rev. B **72**, 214204 (2005).
33. K. Smith and L. F. Mollenauer, "Experimental observation of soliton interaction over long fiber paths: discovery of a long-range interaction," Opt. Lett. **14**, 1284–1286 (1989).
34. E. M. Dianov, A. V. Luchnikov, A. N. Pilipetskii, and A. M. Prokhorov, "Long-range interaction of picosecond solitons through excitation of acoustic waves in optical fibers," Appl. Phys. B **54**, 175–180 (1992).
35. P. J. Thomas, N. L. Rowell, H. M. van Driel, and G. I. Stegeman, "Normal acoustic modes and Brillouin scattering in single-mode optical fibers," Phys. Rev. B **19**, 4986–4998 (1979).
36. R. M. Shelby, M. D. Levenson, and P. W. Bayer, "Guided acoustic-wave Brillouin scattering," Phys. Rev. B **31**, 5244–5252 (1985).
37. D. Milam, "Review and assessment of measured values of the nonlinear refractive-index coefficient of fused silica," Appl. Opt. **37**, 546–550 (1998).
38. P. J. Hardman, P. D. Townsend, A. J. Poustie, and K. J. Blow, "Experimental investigation of resonant enhancement of the acoustic interaction of optical pulses in an optical fiber," Opt. Lett. **21**, 393–395 (1996).
39. E. L. Buckland and R. W. Boyd, "Electrostrictive contribution to the intensity-dependent refractive index of optical fibers," Opt. Lett. **21**, 1117–1119 (1996).
40. E. L. Buckland and R. W. Boyd, "Measurement of the frequency response of the electrostrictive nonlinearity in optical fibers," Opt. Lett. **22**, 676–678 (1997).
41. A. Fellegara, A. Melloni, and M. Martinelli, "Measurement of the frequency response induced by electrostriction in optical fibers," Opt. Lett. **22**, 1615–1617 (1997).
42. A. Melloni, M. Frasca, A. Garavaglia, A. Tonini, and M. Martinelli, "Direct measurement of electrostriction in optical fibers," Opt. Lett. **23**, 691–693 (1998).
43. E. L. Buckland, "Mode-profile dependence of the electrostrictive response in fibers," Opt. Lett. **24**, 872–874 (1999).
44. E. M. Dianov, M. E. Sukharev, and A. S. Biriukov, "Electrostrictive response in single-mode ring-index-profile fibers," Opt. Lett. **25**, 390–392 (2000).
45. S. Afshar V., V. P. Kalosha, X. Bao, and L. Chen, "Enhancement of stimulated Brillouin scattering of higher-order acoustic modes in single-mode optical fiber," Opt. Lett. **30**, 2685–2687 (2005).
46. J. Feng and F. K. Kneubuhl, "Solitons in a periodic structure with Kerr nonlinearity," IEEE J. Quantum Electron. **29**, 590–597 (1993).
47. V. E. Zakharov, "Collapse of Langmuir waves," Zh. Eksp. Teor. Fiz. **62**, 1745–1751 (1972) [Sov. Phys. JETP **35**, 908–914 (1972)].
48. A. S. Davydov, "Solitons in molecular systems," Phys. Scr. **20**, 387–394 (1979).
49. L. Stenflo, "Nonlinear equations for acoustic gravity waves," Phys. Scr. **33**, 156–158 (1986).
50. H. Hadouaj, B. A. Malomed, and G. A. Maugin, "Dynamics of a soliton in a generalized Zakharov system with dissipation," Phys. Rev. A **44**, 3925–3931 (1991).
51. H. Hadouaj, B. A. Malomed, and G. A. Maugin, "Soliton–soliton collisions in a generalized Zakharov system," Phys. Rev. A **44**, 3932–3940 (1991).
52. G. A. Maugin, H. Hadouaj, and B. A. Malomed, "Nonlinear coupling between shear horizontal surface solitons and Rayleigh waves on elastic structures," Phys. Rev. B **45**, 9688–9694 (1992).
53. I. L. Fabelinskii, *Molecular Scattering of Light* (Plenum, 1968).